J Supercond Nov Magn (2012) 25:1297–1301
DOI 10.1007/s10948-012-1598-x

ORIGINAL PAPER

Point-Contact Andreev-Reflection Spectroscopy in Fe-Based Superconductors: Multigap Superconductivity and Strong Electron–Boson Interaction

M. Tortello · D. Daghero · G.A. Ummarino · V.A. Stepanov · N.D. Zhigadlo · J. Karpinski · J. Jiang · R.S. Gonnelli

Received: 6 April 2012 / Accepted: 11 April 2012 / Published online: 28 April 2012

Abstract We performed point-contact Andreev-reflection measurements in $Ba(Fe_{1-x}Co_x)_2As_2$ single crystals ($x = 0.1$, $T_c = 24.5$ K) and $SmFeAsO_{1-x}F_x$ polycrystals ($x = 0.2$, $T_c = 52$ K). The spectra indicate the presence of two superconducting gaps with no line nodes on the Fermi surface, but also feature additional structures related to the electron–boson interaction (EBI). From the spectra, it is possible to extract the characteristic energy Ω_0 of the mediating boson. In Co-doped Ba-122, we obtain $\Omega_0 = 12$ meV that coincides with the spin-resonance energy observed in neutron-scattering experiments. In Sm-1111, $\Omega_0 = 20$ meV fulfils the relation $\Omega_0 = 4.65 k_B T_c$ inferred from neutron-scattering results on other Fe-based superconductors. The strong electron–boson coupling may also explain some anomalies in the PCAR conductance curves (e.g., the excess conductance at high energy) which sometimes prevent a good fit of the curves with models based on constant, BCS-like order parameters.

M. Tortello (✉) · D. Daghero · G.A. Ummarino · R.S. Gonnelli
Dipartimento di Scienza Applicata e Tecnologia, Politecnico di Torino, 10129 Turin, Italy
e-mail: mauro.tortello@polito.it

V.A. Stepanov
P.N. Lebedev Physical Institute, Russian Academy of Sciences, 119991 Moscow, Russia

N.D. Zhigadlo · J. Karpinski
Laboratory for Solid State Physics, ETHZ, 8093 Zurich, Switzerland

J. Jiang
Applied Superconductivity Center, National High Magnetic Field Laboratory, Florida State University, Tallahassee, FL 32310, USA

Keywords Point-contact Andreev-reflection spectroscopy · Symmetry of the order parameter · Strong-coupling superconductivity

1 Introduction

The order parameter (OP) is one of the fundamental quantities in a superconductor, since it determines how the charge carriers couple to form Cooper pairs. In the standard BCS theory for superconductivity, the pairing potential is due to the interaction between electrons and some kind of mediating bosons (phonons in conventional superconductors), is always attractive, does not depend on energy, and is isotropic in space. The constant amplitude of the OP, Δ, is also the "energy gap" in the superconductor. A generalization of this model to include an energy dependence of the OP, as in the Eliashberg theory, allows a proper description of those superconductors, like Pb, where the electron–boson interaction is particularly strong. Further generalizations are needed to account for OPs that are anisotropic or can even change sign to become negative along some directions in the k space (as for the d-wave symmetry) or multiple OPs related to different sheets of the Fermi surface, as in the well-known MgB_2 or probably in high-T_c superconductors under particular conditions [1].

The Fe-based superconductors are likely to present many of these complications at the same time. The proposed interband coupling mechanism based on spin fluctuations allows the opening of multiple nodeless gaps, but also in some cases, the formation of gaps with point nodes or zeros [2], or even with line nodes [3, 4].

One of the techniques that has been more useful to study the number, the amplitude and the symmetry of the

OPs in Fe-based superconductors and in many other materials is point-contact spectroscopy [5]. Here, we report on point-contact Andreev reflection (PCAR) measurements in the electron-doped compounds $Ba(Fe_{1-x}Co_x)_2As_2$ and $SmFeAsO_{1-x}F_x$, which show multiple gaps without line nodes (and compatible with a $s\pm$ symmetry) but also, in the best cases, clear structures related to the strong electron–boson coupling from which the characteristic energy of the boson spectrum can be extracted.

2 Experimental

Here, the point contacts were not made by using the standard needle-anvil technique (in which a very sharp metallic tip is pressed against the sample surface) but by putting a small drop of silver conductive paste on the fresh sample surface. Though the macroscopic area of the Ag contact is rather large (more than 2000 μm^2), the real current injection occurs only here and there, in nanoscale contacts between single Ag grains and the sample surface. Each of these contacts can fulfil the ballistic condition $a < (\ell, \xi)$ ($a =$ contact radius, $\ell =$ electron mean free path, $\xi =$ coherence length), which is necessary to ensure energy-resolved spectroscopy.

3 Results and Discussion

Figure 1 shows an example of temperature dependence of raw conductance curves obtained in a $Ag/BaFe_{1.8}Co_{0.2}As_2$ point contact where the current is injected along the c-axis. Peaks and shoulders are present at about 4 and 9.5 meV, respectively, suggesting the presence of two superconducting gaps. However, additional structures are also present at higher energies that will be discussed later. The curves show a slight asymmetry at all temperatures and the normal state has a large dip at zero bias which gradually fills with increasing temperature up to about 140 K, the temperature at which, in the parent compound, the magnetic state sets in. The inset reports the low-temperature normalized conductance (symbols) here shown only for positive bias. The curve was actually obtained by symmetrization and normalization (i.e., division by the normal-state conductance at T_c) of the raw experimental conductance curve measured at $T = 4.2$ K. Dashed line represents the fit performed within the one-gap, modified [6] Blonder–Tinkham–Klapwijk model [7] generalized to take into account the angular distribution of the injection current at the N/S interface [8]. Solid line is obtained with the same model but now in the two band case [9, 10]. It is clearly visible how the two-band model reproduces better the curve apart from the additional structure at about 16–18 mV. This fact, together with the absence of evident in-plane anisotropy of the spectra [11] and the systematic absence of zero-bias peaks, indicates that the gaps have no line nodes and are presumably almost isotropic (although the existence of point zeros [2] in some small regions of the Fermi surface, as suggested by Raman data [12] cannot be excluded). In the BTK model, gaps are assumed to have an s-wave symmetry. Notice that PCAR cannot discriminate between a $s{+}{+}$ and a $s\pm$ symmetry since it is not sensitive to the sign of the OP (unless a sign change occurs in a region of the same Fermi surface sheet, giving rise to interference effects between hole-like and electron-like quasiparticles, as in the d-wave case).

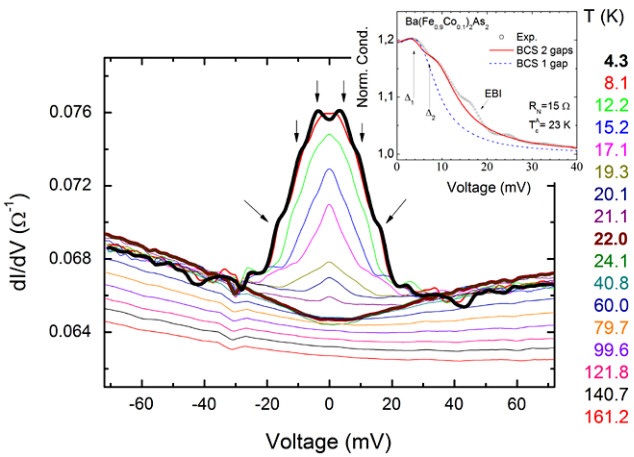

Fig. 1 Temperature dependence of the raw conductance curves measured in a c-axis point-contact on a $Ba(Fe_{1-x}Co_x)_2As_2$ single crystal ($x = 0.1$, $T_c = 24.5$ K). *Inset*: low-temperature normalized conductance curve (*symbols*) compared to the one-band (*dashed line*) and two-band (*solid line*) BTK fit obtained by using BCS-like gaps

The parameters of the best fitting curve, shown in the inset to Fig. 1 are the gaps $\Delta_1 = 4.6$ meV and $\Delta_2 = 9.3$ meV, the broadening parameters $\Gamma_1 = 2.0$ meV and $\Gamma_2 = 4.1$ meV, the barrier parameters $Z_1 = 0.167$ and $Z_2 = 0.367$ (proportional to the height of the potential barrier at the interface) and the weight of the band 1 in the conductance, $w_1 = 0.4$. Similar results were obtained from the fits of various other conductance curves of c-axis contacts; the final average gap amplitudes turned out to be $\Delta_1^c = 4.1 \pm 0.4$ meV and $\Delta_2^c = 9.2 \pm 1.0$ meV. For ab-plane contacts, we got $\Delta_1^{ab} = 4.4 \pm 0.6$ meV and $\Delta_2^{ab} = 9.9 \pm 1.2$ meV. These values correspond to gap ratios $2\Delta_1/k_BT_c \approx 4.3$ and $2\Delta_2/k_BT_c \approx 9.0$, both larger than the BCS value thus suggesting the possibility of moderate- or strong-coupling superconductivity. The small variation in the gap values on changing the direction of current injection confirms that the OPs are likely to be isotropic. Interestingly, also the weight of the two effective bands remains practically the same for current injection along the c axis or along the ab plane. This can be taken as an indirect indication of the fact that the bands in this compound have an almost equal degree of three-dimensionality, as suggested by ARPES [13], x-ray Compton scattering [14], and first-principles calculations [15].

The gap values mentioned above, as well as the critical temperature can be reproduced within an effective three-band $s\pm$ Eliashberg model [16, 17] with a dominant interband coupling between the single hole-like FS sheet around the Γ point of the Brillouin zone and the two electron-like sheets around the M point. The electron–boson spectral function is assumed to be a Lorentzian function peaked at the energy Ω_0. If Ω_0 is chosen to coincide with the spin-resonance energy observed by inelastic neutron scattering measurements [18, 19], i.e., $\Omega_0 = 12$ meV, the model allows obtaining three gaps: $\Delta_1 = 6.1$ meV (hole FS), $\Delta_2 = -3.8$ meV (outer electron FS) and $\Delta_3 = -8.0$ meV (inner electron FS). The calculated T_c is $T_{c,th} = 24.9$ K, taking into account the feedback effect [17]. As shown elsewhere [11], these gap values are compatible with both ARPES [20] and PCARS results, if one assumes that: (i) the ARPES measurements in Ref. [20] actually probed only one of the two electron bands, thus measuring $|\Delta_1| = 7 \pm 1$ meV and $|\Delta_2| = 4.5 \pm 0.6$ meV; (ii) PCARS measurements, if fitted to a two-band BTK model, give mainly $|\Delta_2| = 4.35 \pm 0.65$ meV and $|\Delta_3| = 9.65 \pm 1.45$ meV (averaged over all directions) and do not allow resolving the intermediate gap $|\Delta_1|$.

In addition to the gap structures, the curve in Fig. 1(a) also shows additional features at about 20 meV that are systematically observed in many PCAR spectra with large Andreev-reflection signal (and thus large amplitude). Since they disappear at the critical temperature of the contact, they must therefore be related to some aspects of superconductivity that are not accounted for by the generalized two-band BTK model [5], based on BCS (i.e., energy independent) order parameters, used to fit the data. Within the Eliashberg theory, these structures naturally arise from the energy dependence of the (complex) order parameter, which in turn contains the information on the shape of the electron–boson spectral function $\alpha^2 F(\Omega)$ [5, 11]. Things work in such a way that the sign-changed derivative of the conductance, $-d^2I/dV^2$, shows peaks at the typical boson energies, shifted by the energy gap (in our case, the largest one) [11]. Although in the aforementioned calculations of the energy gap, we have already used a boson spectrum peaked at $\Omega_0 = 12$ meV, the analysis of the electron–boson-interaction (EBI) structures may allow a direct determination of the characteristic boson energy Ω_b. To do so, we calculated the derivative of some experimental PCAR spectra: the resulting curves (Fig. 2(a)) clearly show a main maximum at about $E_p \cong 20$ mV. It is, however, even more interesting to analyze the temperature dependence of such features, as reported in Fig. 2(b) corresponding to the point contact of Fig. 1: on increasing temperature, E_p decreases as shown in Fig. 2(c) (solid symbols). Subtracting the amplitude of the larger gap $\Delta_2 = \Delta_{\max}$ from E_p gives the energy Ω_b (open symbols) where the electron–boson spectral function is expected to show a peak. Both the low-temperature value and the temperature dependence of Ω_b

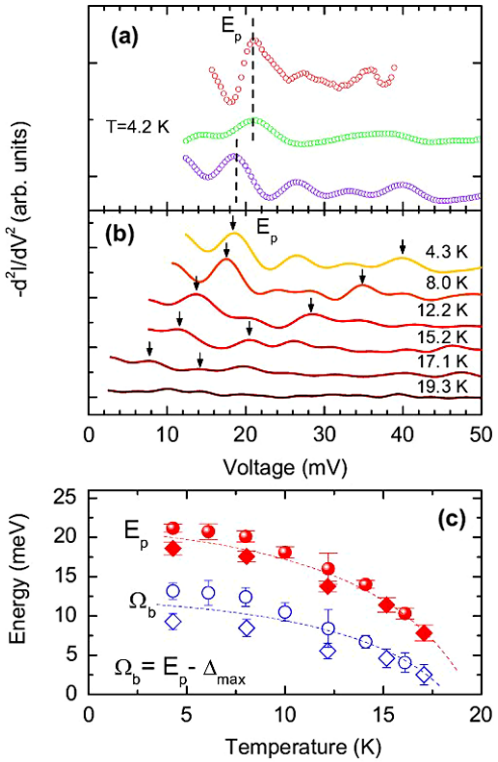

Fig. 2 (**a**) Some examples of sign-changed second derivative $-d^2I/dV^2$ that shows the peaks associated with the strong electron–boson coupling. (**b**) Temperature dependence of the sign-changed second derivative reported in (**a**), bottom curve. (**c**) Temperature dependence of the energy E_p of the main peak in $-d^2I/dV^2$ (*solid symbols*) and of the characteristic boson energy $\Omega_b = E_p - \Delta_{\max}$ (*open symbols*) obtained from the curves in (**b**) (*diamonds*) and from another set of curves (*circles*)

are very similar to those of the energy of the spin resonance observed in $Ba(Fe_{1-x}Co_x)_2As_2$ by neutron scattering experiments [18]. This confirms our choice for Ω_0 in the Eliashberg calculation and strongly supports the $s\pm$ model of superconductivity in Fe-based compounds, where the dominant interband coupling is mediated by spin fluctuations [16, 17].

We will now use the same approach for $SmFeAsO_{1-x}F_x$. Figure 3(a) presents the positive-bias side of a symmetrized conductance curve measured in an almost optimally-doped Sm-1111 polycrystals, namely $SmFeAsO_{0.8}F_{0.2}$. The curve shows a clear maximum at 5 meV and a shoulder at about 16 meV. Both these structures can be ascribed to the presence of two gaps and can indeed be reproduced by a generalized two-band BTK model. The values of the gaps that give rise to the theoretical BTK curve shown in Fig. 2(a) as a dashed line are $\Delta_1 = 6.0$ meV and $\Delta_2 = 19.5$ meV. The broadening parameters are very small, i.e. $\Gamma_1 = 0.1$ meV and $\Gamma_2 = 2.5$ meV, while $Z_1 = 0.20$, $Z_2 = 0.1$ and $w_1 = 0.6$.

Moreover, we can observe that additional structures are also present in this compound at about 27 and 40 meV,

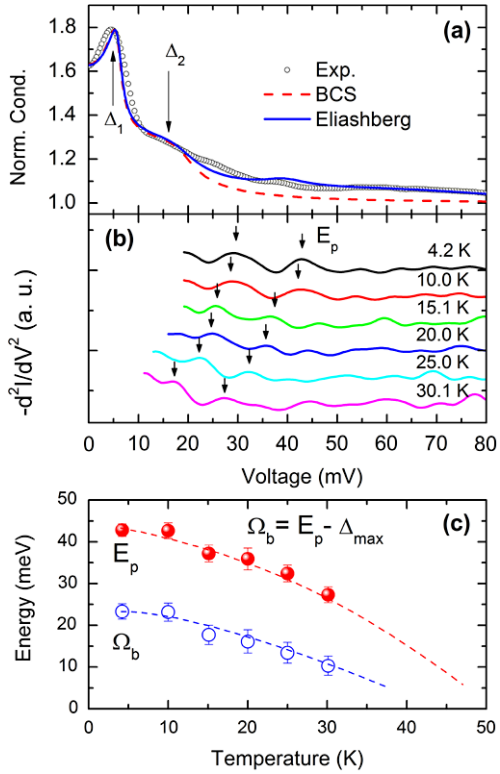

Fig. 3 (**a**) An example of low-temperature normalized conductance curve measured in a point contact on a $SmFeAsO_{1-x}F_x$ polycrystal (*symbols*) compared to the two-band BTK fit obtained by using BCS-like gaps (*dashed line*) and the energy-dependent gaps given by the solution of Eliashberg equations (*solid line*). (**b**) Temperature dependence of the sign-changed second derivative $-d^2I/dV^2$ that shows the peaks associated with the strong electron–boson coupling. (**c**) Temperature dependence of the energy E_p of the main peak in $-d^2I/dV^2$ (*solid symbols*) and of the characteristic boson energy $\Omega_b = E_p - \Delta_{\max}$ (*open symbols*) obtained from the curves shown in (**b**)

which are not reproduced by the BTK model with BCS gaps. By looking at the temperature dependence of the sign-changed second derivative (Fig. 3(b)), of the energy peak, E_p at about 40 meV (solid symbols, Fig. 3(c)) and of $\Omega_b = E_p - \Delta_{\max}$, we can see that the additional structures are most probably related to a strong electron–boson interaction, which we can try to analyze further in the following.

The values of the gaps are well compatible with those presented elsewhere [22] and it is possible to try the same analysis within the three-band $s\pm$ Eliashberg theory, in an analogous way as shown above for Co-doped Ba-122 (but here we have two hole-like bands and one electron-like band) [17]. To the best of our knowledge, no information on the possible presence of a spin-resonance energy is available yet. Nevertheless, if we assume that the relationship $\Omega_0 = 4.65 k_B T_c$, observed in other Fe-based compounds [19], holds in this case, also; it is possible to reproduce the experimentally observed gap values and T_c remarkably well, i.e., $\Delta_1 = 6.03$ meV, $\Delta_2 = 17.23$ meV, $\Delta_3 = -19.56$ meV, and $T_{c,th} = 54.7$ K (taking into account the feedback effect, [17]), using $\Omega_0 = 20$ meV. Now, as a further analysis, we introduce the obtained energy-dependent order parameters into the BTK conductance. The result is shown in Fig. 3(a) as a solid line. The agreement with the experiment is really good. Now, only the additional structure at 27 meV is not reproduced, probably because the actual shape of the electron–boson spectral function is more complicated than a simple Lorentzian one. Notice that the conductance is now better reproduced also in correspondence of the "high-energy tails," i.e., above 50–60 meV. This could not be achieved by the model with BCS gaps, and thus this latter effect could be another manifestation of the strong-coupling character of this compound. Further investigation in this regard is therefore desirable.

4 Conclusions

In conclusion, we have shown that PCAR experiments in $BaFe_{1.8}Co_{0.2}As_2$ single crystals ($T_c = 24.5$ K) and $SmFeAsO_{0.8}F_{0.2}$ polycrystals ($T_c = 52$ K) show clear evidence for multigap, nodeless superconductivity that can be interpreted within a three-band $s\pm$ Eliashberg theory with dominant interband character of the coupling, and thus in agreement with proposed models in Fe-based superconductors [21]. Moreover, additional structures related to strong electron–boson interactions have been observed in both compounds. For the 122 compound the characteristic energy of the mediating boson, $\Omega_0 = 12$ meV, extracted from the measurements, coincides with the spin-resonance energy observed in neutron scattering experiments. For the 1111 superconductor, the extracted boson energy, $\Omega_0 = 20$ meV, fulfils the relationship $\Omega_0 = 4.65\ k_B T_c$, as inferred from neutron scattering experiments on several Fe-based compounds. The related EBI feature can also be reproduced by introducing the energy-dependent order parameters in the BTK conductance. Therefore, these results support a picture where Fe-based are moderate- or strong-coupling superconductors with a spin-fluctuation-mediated mechanism of pairing.

Acknowledgement This work was done within the PRIN Project No. 2008XWLWF9-005.

References

1. Perali, A., Bianconi, A., Lanzara, A., Saini, N.L.: Solid State Commun. **100**, 181 (1996)
2. Mazin, I.I., Devereaux, T.P., Analytis, J.G., Chu, J.-H., Fisher, I.R., Muschler, B., Hackl, R.: Phys. Rev. B **82**, 180502(R) (2010)
3. Kuroki, K., Usui, H., Onari, S., Arita, R., Aoki, H.: Phys. Rev. B **79**, 224511 (2009)
4. Suzuki, K., Usui, H., Kuroki, K.: J. Phys. Soc. Jpn. **80**, 013710 (2011)

5. Daghero, D., Gonnelli, R.S.: Supercond. Sci. Technol. **23**, 043001 (2010)
6. Plecenik, A., Grajcar, M., Beňačka, Š., Seidel, P., Pfuch, A.: Phys. Rev. B **49**, 10016 (1994)
7. Blonder, G.E., Tinkham, M., Klapwijk, T.M.: Phys. Rev. B **25**, 4515 (1982)
8. Kashiwaya, S., Tanaka, Y., Koyanagi, M., Kajimura, K.: Phys. Rev. B **53**, 2667 (1996)
9. Gonnelli, R.S., Daghero, D., Ummarino, G.A., Stepanov, V.A., Jun, J., Kazakov, S.M., Karpinski, J.: Phys. Rev. Lett. **89**, 247004 (2002)
10. Gonnelli, R.S., Daghero, D., Tortello, M., Ummarino, G.A., Stepanov, V.A., Kim, J.S., Kremer, R.K.: Phys. Rev. B **79**, 184526 (2009)
11. Tortello, M., Daghero, D., Ummarino, G.A., Stepanov, V.A., Jiang, J., Weiss, J.D., Hellstrom, E.E., Gonnelli, R.S.: Phys. Rev. Lett. **105**, 237002 (2010)
12. Muschler, B., Prestel, W., Hackl, R., Devereaux, T.P., Analytis, J.G., Chu, J.-H., Fisher, I.R.: Phys. Rev. B **80**, 180510(R) (2009)
13. Vilmercati, P., Fedorov, A., Vobornik, I., Manju, U., Panaccione, G., Goldoni, A., Sefat, A.S., McGuire, M.A., Sales, B.C., Jin, R., Mandrus, D., Singh, D.J., Mannella, N.: Phys. Rev. B **79**, 220503(R) (2009)
14. Utfeld, C., Laverock, J., Haynes, T.D., Dugdale, S.B., Duffy, J.A., Butchers, M.W., Taylor, W., Giblin, S.R., Analytis, J.G., Chu, J.-H., Fisher, I.R., Itou, M., Sakurai, Y.: Phys. Rev. B **81**, 064509 (2010)
15. Mazin, I.I., Schmalian, J.: Physica C **469**, 614 (2009)
16. Ummarino, G.A., Tortello, M., Daghero, D., Gonnelli, R.S.: Phys. Rev. B **80**, 172503 (2009)
17. Ummarino, G.A.: Phys. Rev. B **83**, 092508 (2011)
18. Inosov, D.S., Park, J.T., Bourges, P., Sun, D.L., Sidis, Y., Schneidewind, A., Hradil, K., Haug, D., Lin, C.T., Keimer, B., Hinkov, V.: Nat. Phys. **6**, 178 (2010)
19. Paglione, J., Greene, R.L.: Nat. Phys. **6**, 645 (2010)
20. Terashima, K., Sekiba, Y., Bowen, J.H., Nakayama, K., Kawahara, T., Sato, T., Richard, P., Xu, Y.-M., Li, L.J., Cao, G.H., Xu, Z.-A., Ding, H., Takahashi, T.: Proc. Natl. Acad. Sci. USA **106**, 7330 (2009)
21. Mazin, I.I., Singh, D.J., Johannes, M.D., Du, M.H.: Phys. Rev. Lett. **101**, 057003 (2008)
22. Daghero, D., Tortello, M., Gonnelli, R.S., Stepanov, V.A., Zhigadlo, N.D., Karpinski, J.: Phys. Rev. B **80**, 060502(R) (2009)